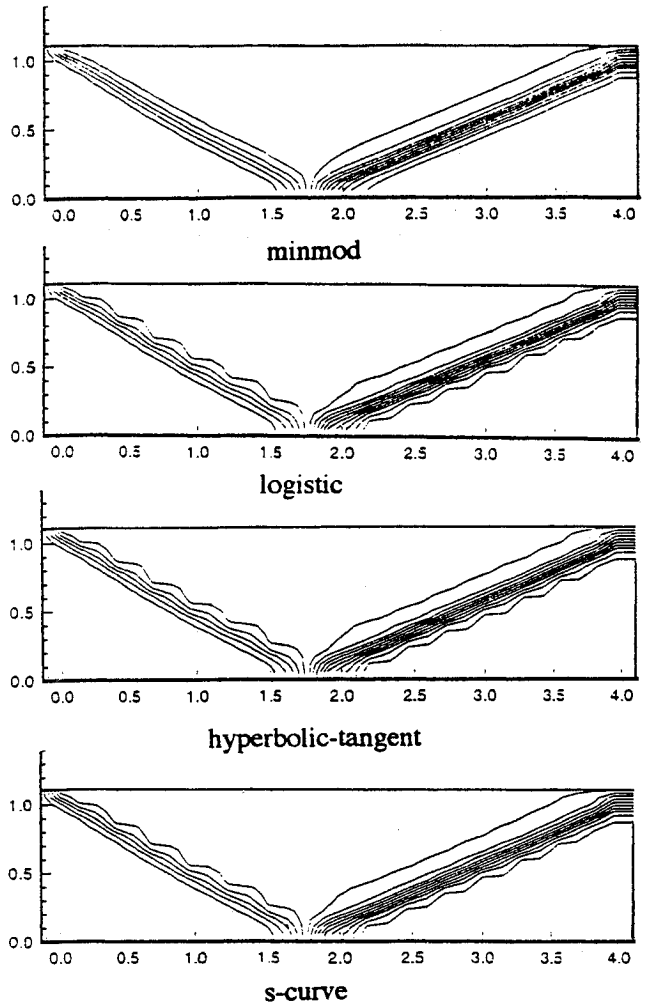

Fig. 1 Shock reflection (pressure plots).

function, which was shown previously, and the hyperbolic-tangent signal function and the logistic signal function, which give, for the hyperbolic-tangent signal function:

$$g_{j+1} = a_{j+1/2}\,[\,(1/2)\tanh(5\{r-1/2\}+1/2)\,]$$

and for the logistic signal function:

$$g_{j+1} = a_{j+1/2}\,[1+e^{-9(r-1/2)}]^{-1}$$

It would be presumptuous of us to assume that we have invented new algorithms for use in CFD. If one refers to the paper by Sweby one sees a priori that each of these signal functions is suitable as a flux limiter. It is the purpose of this Note to point out the connection to fuzzy logic and neural nets and propose possible extensions of this idea.

Results

Several classic flow problems were investigated, including the one-dimensional shock tube and a shock reflection problem. The shock reflection results are presented here since they are most illustrative of the effects of the flux limiters. The conditions of the shock reflection problem is presented in Yee et al.[5] and so only the results will be shown here.

Figure 1 shows pressure contours for the four signal functions on a 32 × 21 mesh. It is interesting to note that the minmod (threshold linear signal function) out performs the other three signal functions in capturing the oblique shock waves. Nevertheless, it is shown in Ref. 6 that all of the simulations are second-order accurate and obey the same stability criteria in practice (although no formal stability analysis was done).

Other results show similar behavior.[6] The minmod signal functions are typically superior to the other signal functions and, in practice, the S-curve signal function typically produces the largest pre- and postshock oscillations. All four signal functions, however, produced practical solutions for each case tested.

Conclusions

In this Note we have outlined a fuzzy logic and neural net interpretation of flux limiters. This interpretation has been used in Harten's second-order TVD scheme to demonstrate the model using four signal functions. Results have shown that the minmod flux limiter is superior to the other three, thus indicating that the discovery of superior flux limiters may not come from the study of fuzzy logic or neural nets. However, the analogy has been successfully demonstrated.

Although no new algorithm has been discovered by the neural net analogy there may be an advantage to this approach in the future. First, it is our belief that an essentially non-oscillatory scheme can be modeled as a multiple-input/multiple-output neural network. Preliminary study shows that there is a clear path in this direction. Second, computer hardware based on neural nets is forthcoming. It may be that flow simulations can effectively make use of these machines by using this analogy. Finally, we hope that this Note fosters some new ideas and interpretations of numerical procedures that may broaden the scope of CFD research.

References

[1]Sweby, P. K., "Flux Limiters," *Numerical Methods of the Euler Equations of Fluid Dynamics*, edited by F. Angrand, A. Dervieux, J. A. Desideri, and R. Glowinski, Society for Industrial and Applied Mathematics, Philadelphia, PA, 1985, pp. 48–65.

[2]Harten, A., "High Resolution Scheme for Hyperbolic Conservative Laws," *Journal of Computational Physics*, Vol. 49, March 1983, pp. 357–393.

[3]Kosko, B., *Neural Networks and Fuzzy Systems: A Dynamical Systems Approach to Machine Intelligence*, Prentice-Hall, Englewood Cliffs, NJ, 1992, Chap. 1.

[4]Geszti, T., *Physical Models of Neural Networks*, World Scientific, Singapore, 1990, Chap. 2.

[5]Yee, H. C., Warming, R. F., and Harten, A., "TVD Schemes," *Numerical Methods of the Euler Equations of Fluid Dynamics*, edited by F. Angrand, A. Dervieux, J. A. Desideri, and R. Glowinski, Society for Industrial and Applied Mathematics, Philadelphia, PA, 1985, pp. 84–107.

[6]Smithwick, Q. Y., "Fuzzy Controller and Neural Network Models for Harten's Second Order TVD Scheme," M.S. Dissertation, Dept. of Aeronautics and Astronautics, Univ. of Washington, Seattle, Washington, 1992.

Application of Singular Value Decomposition to Direct Matrix Update Method

Wai Ming To*
Hong Kong University of Science and Technology, Clear Water Bay, Kowloon, Hong Kong

Nomenclature

$[I]$	= unit matrix
$[K_A]$	= analytical stiffness matrix of a structure
$[M_A]$	= analytical mass matrix of a structure
m	= number of measured modes
n	= number of degrees of freedom in the structural model
r	= number of structural error sites
$[\Delta K_{\text{Baruch}}]$	= Baruch's ΔK matrix
$[\Delta M_{\text{Berman}}]$	= Berman's ΔM matrix
$[\Phi]$	= measured mode shape matrix

Received Jan. 11, 1994; revision received May 16, 1994; accepted for publication May 16, 1994.

*Lecturer, Department of Mechanical Engineering. Member AIAA.

$[\Omega]$ = measured natural frequency matrix
$[\,]^T$ = transpose of a matrix
$\stackrel{\Delta}{=}$ = to be defined as

I. Introduction

In the dynamic analysis of a mechanical or civil structure, structural response data can be obtained analytically by using a finite element model and/or experimentally by performing a modal test on the structure. Experience shows that in general the analytical response data do not match with their experimental counterpart. If that is the case, it is usual practice to update the finite element model based on experimental data using model updating techniques.

Among many model updating techniques, the direct matrix update method developed and investigated by Baruch and Itzhack,[1] Berman,[2] and Wei[3] is one of the most popular techniques and has been incorporated into commercial vibration analysis software. In Ref. 2, Berman employed a Lagrange multiplier technique with a minimum weight-change constraint to obtain a formula in which a high-order (full-order) matrix can be determined by postmultiplying and premultiplying a low-order matrix with two rectangular matrices. In a paper by To and Ewins,[4] it has been shown that these rectangular matrices are the mass-weighted left-inverse of $[\Phi]$ and mass-weighted right-inverse of $[\Phi]^T$, respectively. Therefore, Berman's ΔM matrix would never be an actual mass error matrix when the modal data are incomplete in terms of the number of measured modes and coordinates.

Berman[2] defined a mass error matrix as follows:

$$[\Delta M_{\text{Berman}}] \stackrel{\Delta}{=} [M_A][\Phi][m_A]^{-1}([I]-[m_A])[m_A]^{-1}[\Phi]^T[M_A] \quad (1)$$

where $[m_A] = [\Phi]^T[M_A][\Phi]$.

Although Berman's ΔM matrix is not the actual mass error matrix, there is a close relationship between these two mass error matrices. It is sometimes necessary in practice to understand the relationship between these two matrices or two $n \times n$ subspaces; for example, how close are they, do they intersect, can one be rotated/projected into the other, and so on. In the following section, it can be seen how questions like these can be answered using the singular value decomposition.

II. Mathematical Analysis

The correct mass matrix satisfies the orthogonality relationship

$$[\Phi]^T[\Delta M][\Phi] = [I] - [m_A] \quad (2)$$

Postmultiplying Eq. (1) by $[\Phi]^T$ and premultiplying Eq. (1) by $[\Phi]$, one can obtain

$$[\Phi]^T[\Delta M_{\text{Berman}}][\Phi] = [I] - [m_A] \quad (3)$$

It can be seen that Berman's ΔM matrix can be described as a projection of the actual mass error matrix in an $n \times n$ subspace.

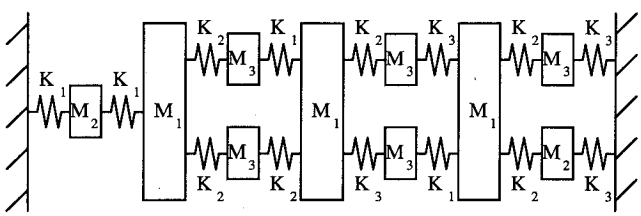

Fig. 1 Lumped spring-mass model with 10 degrees of freedom.

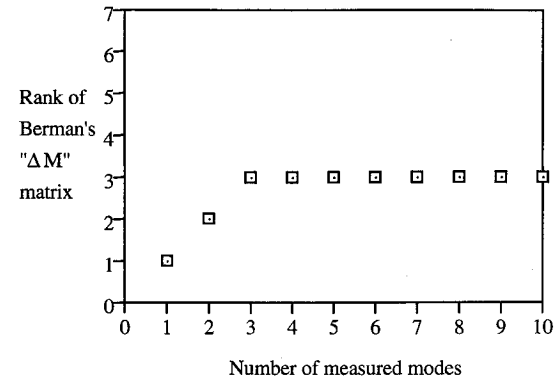

Fig. 2 Rank of Berman's ΔM matrix against the number of measured modes.

From Eq. (1), the rank of $[\Delta M_{\text{Berman}}]$ is smaller than or equal to the minimum value of (rank$[\Phi]$, rank$[M_A]$, rank$([I]-[m_A])$). In all cases, this minimum value is either equal to rank$[\Phi]$ or equal to rank$([I]-[m_A])$, which is smaller than or equal to the minimum value of (rank$[\Phi]$, rank$[\Delta M]$) from Eq. (2). Hence, when the number of measured modes m is smaller than the number of mass error sites r, the rank of Berman's ΔM matrix is smaller than or equal to the number of measured modes m. When the number of measured modes m is equal to or greater than the number of mass error sites r, the rank of Berman's ΔM matrix is smaller than or equal to the number of mass error sites r. Mathematically speaking, it can be stated that for

$$m < r, \ \text{rank}[\Delta M_{\text{Berman}}] \le m \quad \text{(I)}$$

$$m \ge r, \ \text{rank}[\Delta M_{\text{Berman}}] \le r \quad \text{(II)}$$

Alternatively, a comparison of Eqs. (2) and (3) gives

$$[\Phi]^T[\Delta M][\Phi] = [\Phi]^T[\Delta M_{\text{Berman}}][\Phi] \quad (4)$$

which implies the ranks of $[\Phi]^T[\Delta M][\Phi]$ and $[\Phi]^T[\Delta M_{\text{Berman}}][\Phi]$ to be the same and conditions (I) and (II) are justified.

In practice it is more useful to consider the case when the number of measured modes m is equal to or greater than the number of mass error sites r. From Eq. (4), it is shown that

$$\text{rank}([\Phi]^T[\Delta M][\Phi]) = \text{rank}([\Phi]^T[\Delta M_{\text{Berman}}][\Phi]) \quad (5)$$

and Berman's ΔM matrix can be factorized by the singular value decomposition as

$$[\Delta M_{\text{Berman}}] = [U][\Sigma][V]^T \quad (6)$$

Here $[U]$ is an $n \times n$ orthogonal matrix, $[V]$ an $n \times n$ orthogonal matrix, and $[\Sigma]$ a diagonal matrix of rank$[\Delta M_{\text{Berman}}]$ whose nonnegative diagonal elements are the singular values of $[\Delta M_{\text{Berman}}]$.

As a result, in general the rank of $[\Delta M_{\text{Berman}}]$ is equal to the number of mass error sites when the number of measured modes m is equal to or greater than the number of mass error sites r.

Furthermore, conditions (I) and (II) will not be affected by the number of stiffness error sites because Eq. (1) was derived[2] without using the information of system stiffness matrix.

III. Numerical Examples

A 10-degree-of-freedom spring-mass model shown in Fig. 1 was used to check the analysis for a general mass matrix. Three mass errors have been introduced at points 1, 4, and 8 to obtain the measured mode shape matrix. Berman's ΔM matrices were calculated using 1–10 modes for the actual system. The ranks of Ber-

Table 1 Singular values of Berman's ΔM matrices for the second case (noisy data)

Number of measured modes m									
1	2	3	4	5	6	7	8	9	10
0.0219	**0.0390**	**0.0739**	**0.1001**	**0.1001**	**0.1001**	**0.1001**	**0.1001**	**0.1001**	**0.1001**
0.0000	**0.0085**	**0.0134**	**0.0133**	**0.0134**	**0.0250**	**0.0249**	**0.0250**	**0.0250**	**0.0250**
0.0000	0.0000	**0.0029**	**0.0030**	**0.0036**	**0.0058**	**0.0074**	**0.0100**	**0.0198**	**0.0199**
0.0000	0.0000	0.0000	**0.0024**	**0.0025**	**0.0032**	**0.0032**	**0.0036**	**0.0099**	**0.0101**
0.0000	0.0000	0.0000	0.0000	0.0002	0.0003	0.0005	0.0006	0.0007	0.0009
0.0000	0.0000	0.0000	0.0000	0.0000	0.0001	0.0002	0.0005	0.0007	0.0007
0.0000	0.0000	0.0000	0.0000	0.0000	0.0000	0.0001	0.0002	0.0006	0.0006
0.0000	0.0000	0.0000	0.0000	0.0000	0.0000	0.0000	0.0001	0.0003	0.0003
0.0000	0.0000	0.0000	0.0000	0.0000	0.0000	0.0000	0.0000	0.0001	0.0001
0.0000	0.0000	0.0000	0.0000	0.0000	0.0000	0.0000	0.0000	0.0000	0.0001

man's ΔM matrices were determined by the singular value decomposition and are plotted in Fig. 2, where it can be seen that the rank of Berman's ΔM matrix was 3 when three or more measured modes were available.

The second case study was carried out on the same analytical model. In this case mass errors at points 2, 3, 5, and 8 and stiffness errors between points 2 and 3, 5 and 6, and 6 and 7 have been introduced. Berman's ΔM matrices were calculated using 1–10 modes for the actual system and their ranks were determined by the singular value decomposition. Again, the rank of Berman's ΔM matrix was equal to the number of mass error sites when sufficient (four or more) measured modes were available and was not affected by the number of stiffness errors made on the structure. Table 1 shows the singular values of Berman's ΔM matrix when the measured mode shape vectors were contaminated by 2% Gaussian random error. It can be seen that the numerical rank was 4 when four or more measured modes were available. A careful definition of numerical rank has been given in a paper by Golub et al.[5] The essential idea is briefly described as follows. We were going to look at the nonzero singular values of Berman's ΔM matrices and chose a number δ as a zero threshold. The choice of δ was based on measurement errors (information about the uncertainty of the measured data) incurred in estimating the coefficients of those Berman ΔM matrices. In this case 2% random error was applied to the measured mode shape vectors so that by considering the roundoff and the measurement errors in the matrix computation the value of δ was set to 0.02 times the spectral norm of Berman's ΔM matrix.

IV. Concluding Remarks

It is proved that in general Berman's ΔM matrix is a projection of the actual mass error matrix in an $n \times n$ subspace when sufficient modes are available. And so the number of mass error sites can be determined when Berman's ΔM matrix is factorized using the singular value decomposition. This technique would not be affected by the number of stiffness errors for any system. If the measured mode shape vectors are slightly contaminated by measurement noise, the numerical rank can be used as an indicator for the number of mass error sites. The noise introduced in the measurement of natural frequencies will not affect the determination of Berman's ΔM matrix and hence has no effect of its rank.

On the contrary, Baruch's ΔK matrix is able to determine the rank of an actual stiffness error matrix only when sufficient modes are available and the correct mass matrix is used. This is because Baruch[1] derived his formula using a known symmetric positive definite mass matrix, so inherently the correct mass matrix was used to obtain the Baruch's ΔK matrix. His formula for a stiffness error matrix is given as follows:

$$[\Delta K_{\text{Baruch}}] \triangleq -[K_A][\Phi][\Phi]^T[M_A] - [M_A][\Phi][\Phi]^T[K_A] + [M_A][\Phi][\Phi]^T[K_A][\Phi][\Phi]^T[M_A] + [M_A][\Phi][\Omega][\Phi]^T[K_A]$$

From the preceding equation, one can observe that if both sets of measured natural frequencies and mode shape vectors are contaminated by measurement noise, the rank of Baruch's ΔK matrix may be affected.

Acknowledgments

The author gratefully acknowledges the financial support of the Croucher Foundation in Hong Kong. He also wishes to thank D. J. Ewins at Imperial College for supervising this work.

References

[1]Baruch, M., and Itzhack, I. Y. B., "Optimal Weighted Orthogonalization of Measured Modes," *AIAA Journal*, Vol. 16, No. 4, 1978, pp. 346–351.

[2]Berman, A., "Mass Matrix Correction Using an Incomplete Set of Measured Modes," *AIAA Journal*, Vol. 17, No. 10, 1979, pp. 1147, 1148.

[3]Wei, F. S., "Stiffness Matrix Correction from Incomplete Test Data," *AIAA Journal*, Vol. 18, No. 10, 1980, pp. 1274, 1275.

[4]To, W. M., and Ewins, D. J., "A Criterion for the Localization of Structural Modification Sites Using Modal Data," *Proceedings of the 8th International Modal Analysis Conference*, Vol. 2, 1990, pp. 961–967.

[5]Golub, G. H., Klema, V. C., and Stewart, G. W., "Rank Degeneracy and Least Squares Problems," Dept. of Computer Science, Stanford Univ., Tech. Rept. STAN-CS-76-559, Stanford, CA, Aug. 1976.

Space Shuttle Main Engine Sensor Modeling Using Vector Quantization

Timothy F. Doniere* and Atam P. Dhawan†
University of Cincinnati, Cincinnati, Ohio 45221

Introduction

ARTIFICIAL neural networks have been used to model Space Shuttle main engine (SSME) sensor parameters.[1,2] A neural network sensor model predicts the value of the sensor parameter based on a selected set of other sensor measurements. The errors, or differences between the values predicted by the model and the actual sensor values, provide information on the health of the sensor.

Developing accurate models is particularly difficult due to the highly complex, nonlinear nature of SSME, the limited suite of measured parameters, and the large variability of behavior among engines of the same design. Neural networks are well suited for problems in which the exact relationships between inputs and outputs are complex or unknown, if the system state is sufficiently represented in the inputs.[3] Feedforward neural networks have been effectively used to model critical parameters of the SSME during the startup transient.[4]

Received Oct. 1, 1993; revision received April 14, 1994; accepted for publication April 15, 1994.

*Graduate Student, Electrical and Computer Engineering Department.

†Associate Professor, Electrical and Computer Engineering Department, Rhodes Hall, ML30.